THE JOURNAL OF PHYSICAL CHEMISTRY C

Article

pubs.acs.org/JPCC

Resonant Inelastic X-ray Scattering of Molybdenum Oxides and Sulfides

Rowena Thomas,[†,‡] Josh Kas,[§] Pieter Glatzel,[⊥] Mustafa Al Samarai,[#] Frank M. F. de Groot,[#] Roberto Alonso Mori,[⊥,∥] Matjaž Kavčič,[○] Matjaz Zitnik,[○] Klemen Bucar,[○] John J. Rehr,[§] and Moniek Tromp*[,‡]

[†]University of Southampton, Southampton, SO17 1BJ, U.K.

[‡]Catalyst Characterisation, Chemistry Department, Catalysis Research Center, Technische Universität München, Ernst-Otto-Fischer-Straße 1, 85748 Garching, Germany

[§]Department of Physics, University of Washington, Seattle, Washington 98195, United States

[⊥]European Synchrotron Radiation Facility (ESRF), BP 220, 38043, Grenoble, Cedex 9, France

[∥]LCLS, SLAC National Accelerator Laboratory, Menlo Park, California 94025, United States

[#]Inorganic Chemistry & Catalysis, Debye Institute for Nanomaterials Science, Utrecht University, Universiteitsweg 99, Utrecht, 3584 CG, Netherlands

[○]J Stefan Institute, SI-1001, Ljubljana, Slovenia

Supporting Information

ABSTRACT: Molybdenum oxides and sulfides were studied using resonant inelastic X-ray scattering (RIXS). The $2p_{3/2}3d$ Mo RIXS planes show a rich structure with considerably more spectral information than in conventional X-ray absorption near edge structure (XANES) spectroscopy. The spectra were simulated using FEFF9 giving generally good agreement and detailed electronic information can be derived. The reference materials serve as a starting point for detailed electronic and geometric investigations of a broad range of compounds. In particular, this can provide insights in the properties and performance of unknown and changing materials like those in catalysis.

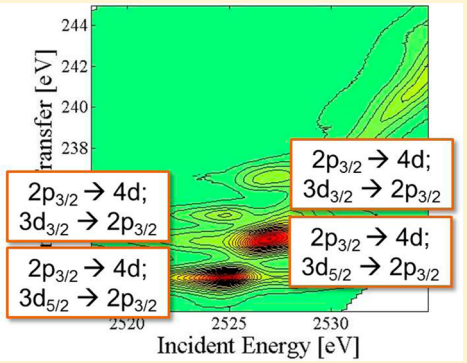

INTRODUCTION

Resonant inelastic X-ray scattering (RIXS) is a powerful tool in studying the electronic density of states while offering high spectral resolution.[1,2] It directly probes the unoccupied and occupied density of states, usually studied by X-ray absorption spectroscopy (XAS) and X-ray emission spectroscopy (XES) respectively. The intensities are measured as a function of incident and emitted photon energies, in the X-ray absorption near edge (XANES) region, identifying their interdependencies and thereby uncovering additional features. It has already been applied successfully for the 3d transition metal complexes,[3] where it has been used to reveal much greater detail in the K edge spectral shape[4] and thereby revealing information on, for example, the metal oxidation state, the local symmetry and crystal field splittings.[6] There are however far fewer studies on 4d or 5d metal systems.[1,5]

In a RIXS experiment a secondary spectrometer with an energy bandwidth similar to the lifetime broadening is used to selectively measure the emission energy.[6] This allows the superior resolution seen in RIXS compared to normal XANES, since the broadening of the spectra is governed by the final state lifetime, rather than the initial state lifetime. For the Mo Lα RIXS as used in this work, emission spectra are recorded at incident energies along the L_3 edge region. The transitions involved are shown in Figure 1 as an energy level diagram. We are looking at the absorption of a photon, of energy Ω, which promotes an electron from a 2p orbital to the 4d shell, creating a $2p_{3/2}4d^{n+1}$ intermediate state. An electron from the 3d shell then drops down to fill the core hole, emitting a photon of energy ω as it does so, and leaving a 3d hole in the final state. The spectra cover the M_4 and M_5 emission edges, so the $3d_{3/2}4d^{n+1}$ and $3d_{5/2}4d^{n+1}$ final states, respectively. The difference between this final state and the initial state is the overall energy transfer of the system. The data is generally presented as a 2D contour plot, with the energy transfer plotted against the incident energy so that both are relative to the ground state.

Received: September 16, 2014
Revised: January 6, 2015
Published: January 7, 2015

DOI: 10.1021/jp509376q
J. Phys. Chem. C 2015, 119, 2419−2426

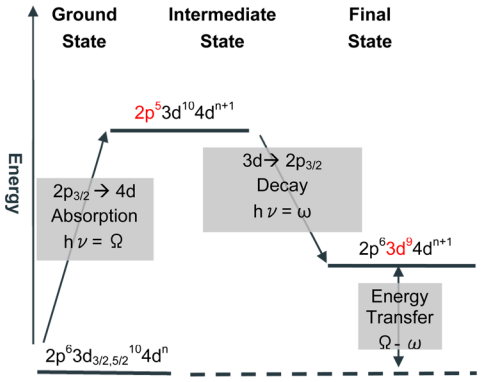

Figure 1. RIXS energy scheme for 2p3d RIXS. The vertical axis represents the energy of the electron configuration. For simplicity only the shells which are changing in configuration are shown.

There have been an increasing number of studies on 3d transition metal RIXS[7,8] but as yet there are no examples of 4d transition metal RIXS in the literature, mainly due to the relative inaccessibility of the energies involved. The L edges of 4d transition metals lie between 2000 and 4000 eV: These soft X-rays require the use of vacuum or reduced/changed atmosphere (e.g., He) sample chambers in order to carry out experiments, since only a few centimeters of air absorb most of the photons. The advantage with studying the L edge as compared to K edge is that we are directly probing the 4d valence shell. The spectra will be much sharper than a conventional L-edge XANES spectrum due to the reduced lifetime broadening of a 3d core hole compared to a 2p core hole. The lifetime of the intermediate $2p_{3/2}$ core hole broadens the spectrum in the incident energy axis only. Broadening of the spectra in the emission or energy transfer direction is due to the final state lifetime, i.e. the lifetime of the 3d hole, which is much shorter and only 0.16 eV for a $3d_{3/2}$ and 0.14 eV for a $3d_{5/2}$ core hole compared to 1.74 eV for a $2p_{3/2}$ hole. We may also see different features in the RIXS compared to the XANES as this is a two-step process compared to a one step p to d transition for L-edge XANES, so different symmetry operations are active.

There are L-edge molybdenum XANES studies in the literature, particularly for the metal oxides,[9,10] and these provide an interesting comparison to look for any additional effects in the RIXS. The L-edge XANES spectra all show a characteristic "white line" due to the dipole allowed 2p to 4d transition, and the splitting of this peak can be directly related back to the coordination geometry (for simple geometries).[11−13]

Figure 2 shows examples of molybdenum L_3-edge XANES spectra[14] and it can be seen that for the sodium molybdate, with the central Mo atom in a tetrahedral environment, the intensity ratio is approximately 2:3, whereas for the molybdenum(III) oxide (octahedral) the intensity ratio is reversed and the first peak is of greater intensity. This is consistent with similar studies in the literature. This peak results from the 2p to 4d transition so the splitting relates directly to the crystal field splitting and the intensity ratios of the two peaks give a measure for the orbital distribution and thus geometry (Figure 3).

The charge transfer multiplet theory[15,16] has been successful in modeling the L-edge XAS of mainly 3d transition metals. This theory models the metal complex using crystal field theory and takes into account the multiplet effects present, i.e. the interactions of the core hole and the valence electrons.

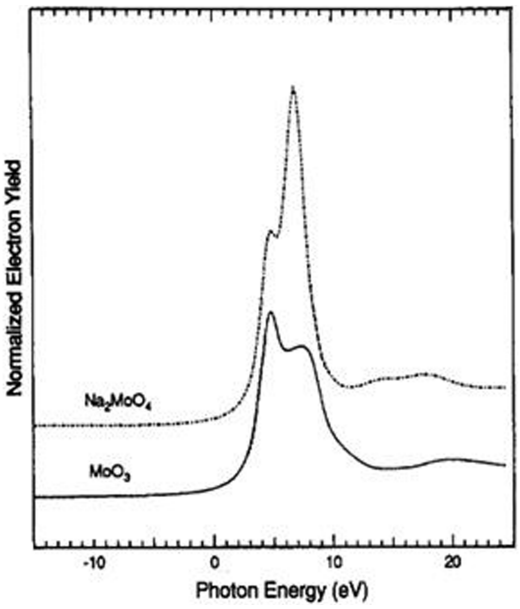

Figure 2. Normalized fluorescence yield Mo L_3-edge XANES taken from Hu and Wachs.[14] Reprinted from ref 14. Copyright 1995 American Chemical Society.

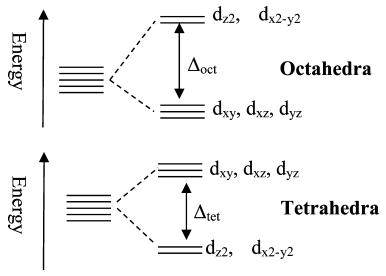

Figure 3. Energy level diagram showing d-orbital crystal field splitting for octahedral and tetrahedral environments.

Moreover, charge transfer and electron transfer correlations can be accounted for, when necessary. The Mo L-edge XANES spectra of the 4d transition metal Mo systems Na_2MoO_4 and $(NH_4)_2MoS_4$ have been simulated well using the multiplet approach, despite these being very covalent systems.[9] An extensive L_2 and L_3 edge XAS study on octahedral 3d and 4d metals,[17] including Mo, has demonstrated that for 4d transition metals the 2p spin−orbit coupling is large and an L_3:L_2 intensity ratio of ∼2:1 is observed. It is shown that pd and dd multiplet effects and 4d spin−orbit coupling are causing the difference between L_3 and L_2, with the L_2 being the least affected by multiplet effects and thus most suitable for single particle simulation techniques (like the FEFF technique as used here, *vide infra*). Since our main goal is to develop RIXS as a tool in (organometallic) catalysis, we aim to obtain insights in the origin of the different features observed. This understanding, including their dependence on structure and electronic properties, will help us to interpret the RIXS planes of unknown and changing structures, thereby providing property-performance relationships on working catalysts. The FEFF9[18] approach, which allows the calculation of full structural models in contrast to the point group calculation with the multiplet theory, is therefore the chosen method here to simulate the experimentally obtained Mo L_3 edge RIXS spectra, although it is based on full potential approach and

DOI: 10.1021/jp509376q
J. Phys. Chem. C 2015, 119, 2419−2426

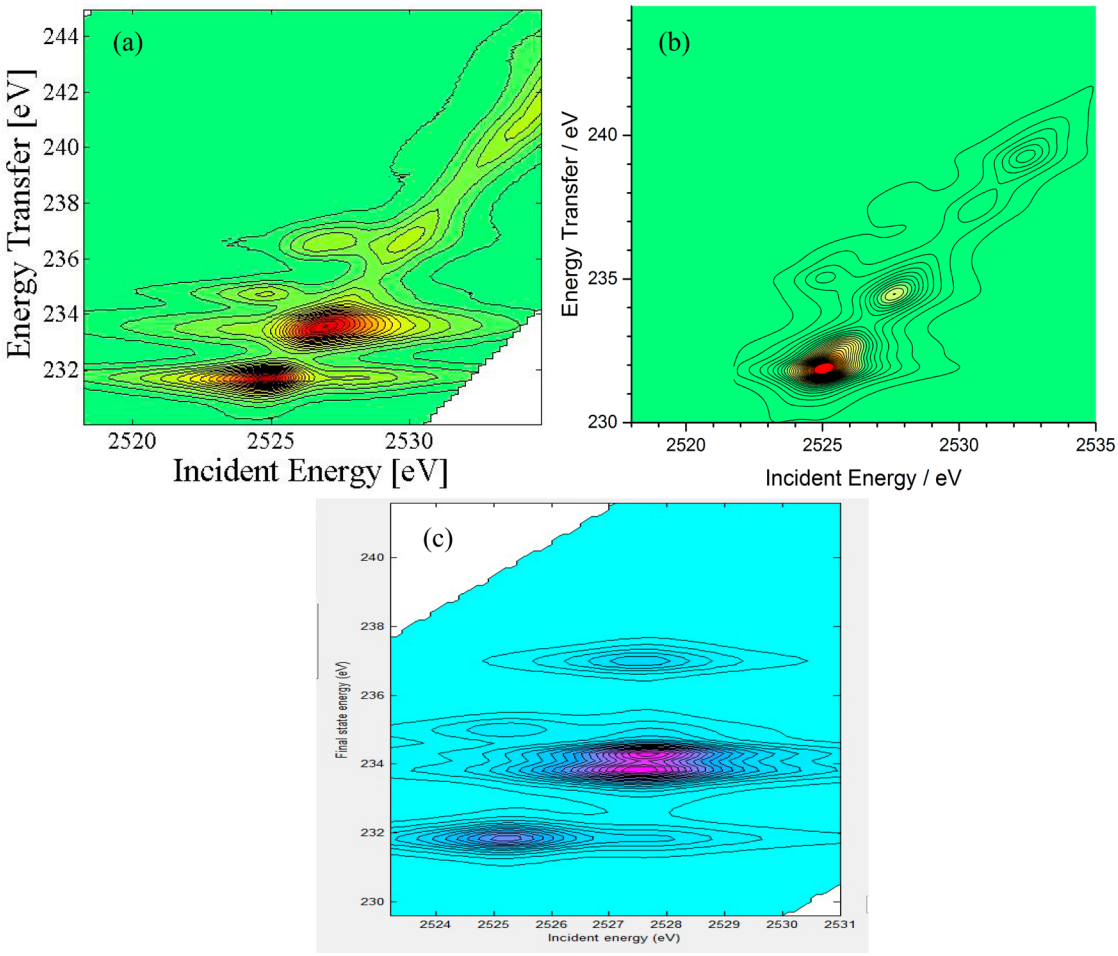

Figure 4. Experimental Lα_1 RIXS plot (a) for Na_2MoO_4 with theoretical RIXS plot calculated using FEFF9 (b) and the CTM4XAS multiplet code (c) for the same compound.

multiplet effects are not included. However, as shown in this paper, recent and ongoing developments make FEFF into a useful and reliable tool for the simulation of RIXS data.[18] The effect of multiplets for the RIXS experiments as performed in this study is checked using the multiplet approach[15,16] and thereby the validity of the use of FEFF evaluated.

We present the theoretical spectra calculated using the real space Green's function (RSGF) code FEFF9[18] for a range of molybdenum Lα RIXS spectra. The specific code used in this work includes a new theoretical treatment of RIXS based on a real-space multiple-scattering Green's function formalism, and includes the effects of both intermediate and final state core-hole interactions. Additional many-body effects can be included via a convolution of the single particle spectrum with an effective spectral function, however in the present article, we have neglected these effects. This new method allows us to simulate these spectra successfully for the first time using a convolution of an effective XAS spectrum and the XES spectrum of the complexes simply based on their crystal structures. Detailed electronic information, i.e., d orbital occupancy and energy splitting, has been derived for these reference materials and the knowledge obtained on the interpretation of the RIXS data will be extremely useful when going to less defined materials. The number of peaks present, their intensity ratios, and the splitting between them can reveal structural and electronic information for unknown compounds, which is desirable for changing catalyst structures, where this information cannot be obtained otherwise.

EXPERIMENTAL SECTION

Molybdenum(IV) oxide, molybdenum(VI) oxide, molybdenum(IV) sulfide, and sodium molybdate were purchased from Sigma-Aldrich.

The 2p3d RIXS spectra were recorded at ID26 of the European Synchrotron Radiation Facility (ESRF), Grenoble, France, across the molybdenum L_3 edge. A cryogenically cooled fixed-exit beamline monochromator consisting of a pair of Si crystals in the (111) reflection was used ($\Delta E/E = 1.4 \times 10^{-4}$). The incoming flux was 10^{13} photons/s. Higher harmonics were suppressed by Si mirrors working under grazing incidence condition.

A complete in-vacuum curved-crystal X-ray emission spectrometer[19] in Johansson geometry was used in collecting these spectra. The first order reflection of a Si(111) crystal was employed in the spectrometer. The sample was positioned inside the Rowland circle rendering a dispersive geometry. A CCD camera was used to collect the spectra. The full RIXS plane consists of 69 consecutive 2p3d RIXS spectra recorded over an incident energy range of 2518 to 2535 eV with a step size of 0.25 eV. The acquisition time for a single RIXS spectrum was 60 s. The maximum count rate was 600 counts/s and occurred at the peak of the Mo Lα1 emission line, excited at 2525 eV (first resonance). The high spatial resolution of the

DOI: 10.1021/jp509376q
J. Phys. Chem. C 2015, 119, 2419−2426

detector yields an absolute spectrometer energy bandwidth of 0.35 eV at the Mo L edge.[19]

The energy calibration of the spectrometer emission energy was done relative to the Lα line measured on a Mo foil, using the absolute nominal crystal 2d lattice spacing and crystal detector distance. For the excitation energy axis the nominal values given by the monochromator were considered. Alternatively, the elastic scattering peak can be used for a relative calibration between spectrometer and monochromator. Between the two approaches a shift of up to ∼1 eV in the emission (final state) energy was observed. Although the possible shift is of course systematic and the same for all samples studies here, it has to be taken into account when comparing these results to other experiments.

FEFF9 was used to model the experimental RIXS spectra and to determine the density of states. FEFF calculations were carried out using a self-consistent field approximation of 8 Å and a full multiple scattering radius of 10 Å around the central Mo atom. Both dipole and quadrupole contributions were included in the calculations. A ground state potential model and a RPA screened core hole were used. The EXCHANGE card was used to reduce the spectral broadening to match the experiment. Crystal structures from the literature were used. Core-hole broadenings for the M_4 and M_5 edges were taken from the literature.[20] A ratio of 9:1 was used for the L_3 edge spin orbit coupling, i.e., $2p_{3/2} \rightarrow 3d_{5/2} = 9$, $2p_{3/2} \rightarrow 3d_{3/2} = 1$, as expected based on transition probabilities. In case different Mo sites are present in the structure, the simulated data represent an average of all.

Multiplet calculations were performed using the CTM4XAS program, with parameters as indicated in the text.[21]

RESULTS

Figure 4 shows the experimental Lα RIXS spectrum for Na_2MoO_4 as a contour plot (a) alongside the theoretical plot for the same compound as calculated by FEFF9 (b) and the CTM4XAS multiplet code (c).

The main peak is split in 2 along the diagonal, with maxima at 2524.75 eV incident energy and 231.66 eV energy transfer and at 2527.00 eV incident energy and 233.5 eV energy transfer. This corresponds to the ligand field splitting of the 4d orbitals. The structure is approximately repeated along a second diagonal shifted with respect to the first by ∼3 eV toward larger energy transfer. The two diagonals are due to the 3d spin−orbit coupling where the stronger spectral features (at lower energy transfer energy) arise from the $3d_{5/2}$ final state. Theoretically the intensity ratio of the 3d spin orbit coupling is calculated as 9:1, with the second diagonal much lower in intensity as in the experiment.

The main peaks along the diagonal can be compared to the L_3 absorption edge spectrum as shown in Figure 2. In the XANES spectrum, the intensity is higher for the lower energy peak; this is evident in the RIXS plots also, when taking into account both the area of the peak and the intensity. In the RIXS plot the peaks are fully separated, in contrast to the overlapping peaks in the normal L edge experiment, and their positions and intensities can thus be better identified. The long tails in the horizontal direction and the sharp tails in the vertical direction indicates that the lifetime broadening in the 3d final state is much reduced compared to the 2p intermediate state. As a consequence the peak positions can be determined with more accuracy. A very important consequence for applications is that the sharper structures will make it easier to separate systems with multiple sites/symmetries/valences.

Along the energy transfer axis we see the spin orbit coupling of the 3d band, the lower energy transfer peaks are due to $3d_{5/2}$ emission, the higher energy transfer peaks are due to emission from $3d_{3/2}$; both are due to $2p_{3/2}$ to 4d absorption. So we can assign the peak at 2524.75 eV incident energy and 231.66 eV energy transfer to the $2p_{3/2}$ to 4d; $3d_{5/2}$ to $2p_{3/2}$ transitions. The peak at 2524.75 eV incident energy and 234.80 eV energy transfer is again caused by $2p_{3/2}$ to 4d absorption, but with $3d_{3/2}$ to $2p_{3/2}$ emission. The energy transfer difference between these two features is approximately 3.12 eV, which corresponds to the spin−orbit coupling of the 3d band, generally found around 3.2 eV.[22] The peak at 2527.00 eV incident energy and 233.54 eV energy transfer is again caused by the $2p_{3/2}$ to 4d and $3d_{5/2}$ to $2p_{3/2}$ transitions, but it is at higher energies due to the splitting of the 4d band. We see another peak at the same incident energy but at ∼3 eV higher in energy transfer, again due to 3d spin orbit coupling.

The plots show that the higher energy transfer transitions are less intense than the peaks at lower energy transfer; this is mainly due to the smaller transition probability of M_4 (0.09) compared to M_5 (0.89). The lifetime broadening of M_4 compared to M_5 is 0.16 eV compared to 0.14 eV, so that effect will be minimal—this is accounted for in the theoretical calculations.

The RIXS is simulated well using the FEFF9 approach. The problem is that the peak intensity ratios along the diagonal are different compared to the experiment. The density of states as calculated and from which the RIXS plane is simulated is shown in Figure 5. A degree of hybridization can be seen between the unoccupied molybdenum d-orbitals and the unoccupied oxygen p-orbitals, as well as a small Mo p contribution.

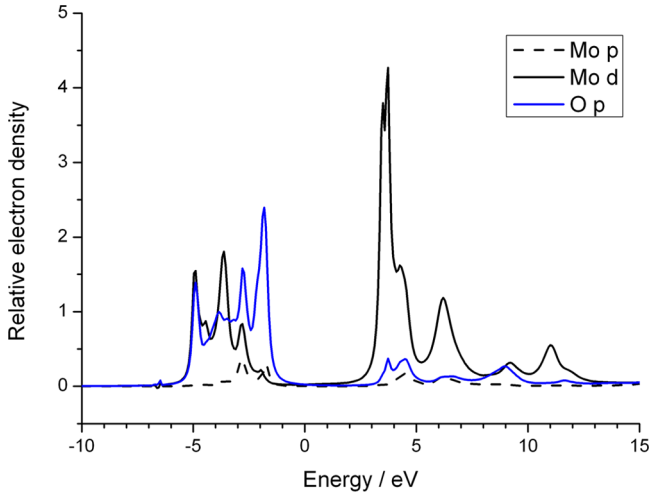

Figure 5. Density of states plot for Na_2MoO_4 as calculated by FEFF9.

We have also calculated the 2p3d transitions with the CTM4XAS multiplet code, using linear polarized X-rays and 90 deg horizontal scattering, a crystal field of −2.1 eV. Figure 4c shows the result for the L_3 edge. The two crystal field split states are visible at 2525.2 and 2527.5 eV. The crystal field splitting is maintained in the $3d^9 4d^1$ final state and the two final state crystal field split states are visible at 232 and 234.3 eV. The effects of the 3d spin−orbit coupling automatically appear (in the correct ratio of 9:1) for multiplet calculations and the

DOI: 10.1021/jp509376q
J. Phys. Chem. C 2015, 119, 2419−2426

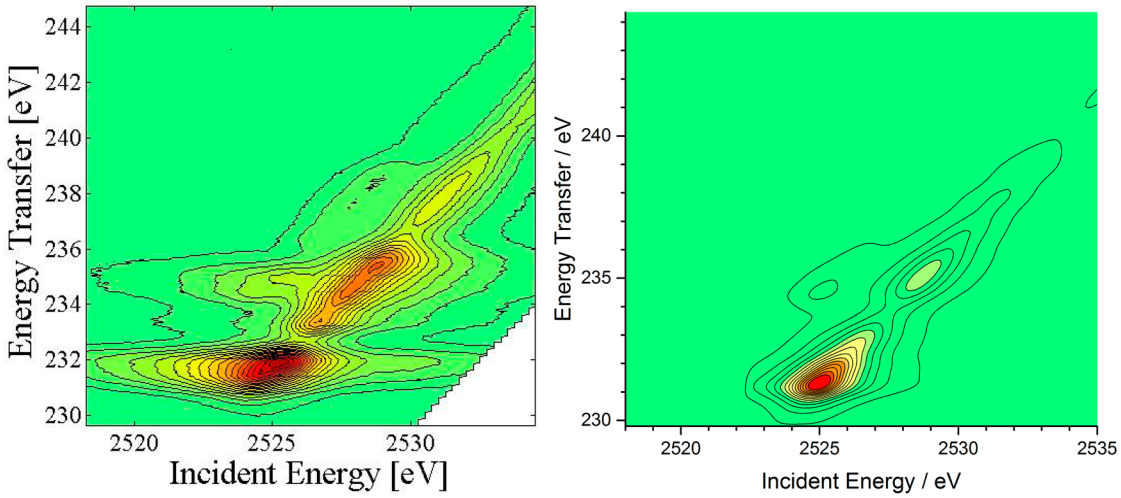

Figure 6. Experimental Lα RIXS plot (left) for MoO_3 with theoretical RIXS plot calculated using FEFF (right) for the same compound.

spin−orbit shoulders are visible at 235 and 237 eV. Apart from this spin−orbit effect, the only visible multiplet effect in the 2D image is the splitting of the peak at (2527.5, 234) eV, which is caused by the 3d4d multiplet interaction in the final state, where we have used values that are 50% of the atomic values (based on previous L edge work suggesting that Mo^{4+} and Mo^{6+} have 50% reduced Slater integrals[17]). With the present resolution, this splitting is not visible in experiment, which suggests that the 3d4d multiplet effects are further reduced. A small broadening of the second peak in energy transfer is visible, which could be a sign of multiplet effects, where we note that an alternative interpretation could be that there are band effects that give a broadening of this peak (see the constant incident energy line scans extracted at 2525 and 2527 eV respectively, Figure S1). An interesting result, which we are not able to explain, is that the CTM4XAS calculation underestimates the first peak with respect to experiment, while the FEFF calculation overestimates the intensity of the first peak.

Because the present data does mainly show the 4d crystal field and the 3d spin−orbit coupling, while the 3d4d multiplet effect does not seem visible, we have for the other experiments only compared them with FEFF calculations.

In Figure 6, we present the experimental and calculated Lα RIXS spectra for MoO_3 as 2D contour plots. The main peak occurs at 2525.25 eV incident energy and 231.90 eV energy transfer. The second peak consists of two features, both along the diagonal. One is at 2527.25 eV incident energy and 233.65 eV energy transfer, the other at 2529.00 eV incident energy and 235.52 eV energy transfer. These can both be attributed to the $2p_{3/2}$ to 4d; $3d_{5/2}$ to $2p_{3/2}$ transitions, with 4d splitting. There are off diagonal peaks which are ∼3 eV higher in the energy transfer direction than the main peaks. These are due to $3d_{3/2}$ to $2p_{3/2}$ emission. We see extra splitting in the main peaks because the Mo atom is not in a perfect octahedral environment, so there is hybridization of orbitals causing extra transitions. For lower symmetries there will be more splitting of the 4d band due to increased orbital hybridization.

The experimental and theoretical plots for molybdenum(VI) oxide again show generally good correlation in the number, relative position and splitting of peaks. For example the splitting of the peaks between 234 and 236 eV energy transfer is reproduced in the RIXS plot calculated by FEFF. The off-diagonal peaks are also both present and the positions as well as intensity ratios are in good agreement. The origin of all peaks can be derived using the density of states calculations, as shown in Figure 7. Significant hybridization of the Mo d and O p unoccupied orbitals is also observed, for all features present.

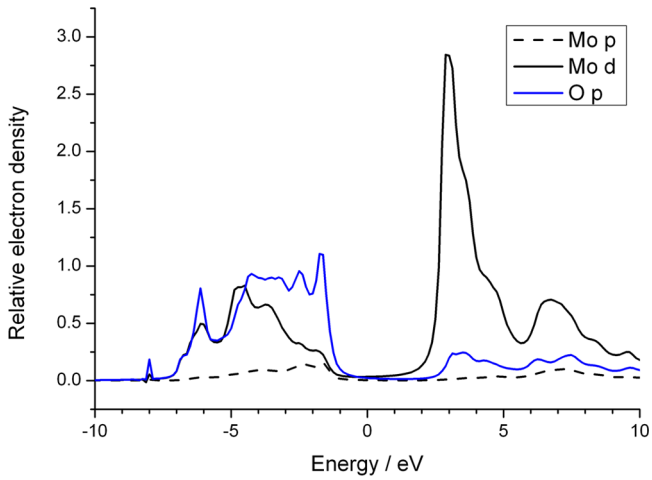

Figure 7. Density of states for MoO_3 as calculated by FEFF9.

In Figure 8, the experimental and theoretical Lα RIXS spectra for MoO_2 as 2D contour plots are shown. MoO_2 has a distorted rutile bulk structure so the molybdenum atoms are in distorted octahedral geometry. It has an unusual feature for a molybdenum oxide; a short metal−metal bond (∼2.5 Å).[23] The main peak along the diagonal is split, due to 4d splitting, with the peak of one feature at 2522.75 eV incident energy and 229.62 eV energy transfer ($2p_{3/2}$ to 4d; $3d_{5/2}$ to $2p_{3/2}$) and the other at 2525.50 eV incident energy and 232.26 eV energy transfer ($2p_{3/2}$ to 4d; $3d_{5/2}$ to $2p_{3/2}$). There are low intensity off-diagonal peaks approximately 3−3.3 eV above main peaks in energy transfer, which corresponds to the 3d spin orbit coupling.

The density of states is shown in Figure 9 and shows hybridization between the Mo d and O p unoccupied orbitals, for all orbitals probed.

The central molybdenum atom in MoS_2 is surrounded by six sulfur atoms in a trigonal prismatic geometry.[24] The overall structure is hexagonal. Figure 10 shows the experimental Lα

DOI: 10.1021/jp509376q
J. Phys. Chem. C 2015, 119, 2419−2426

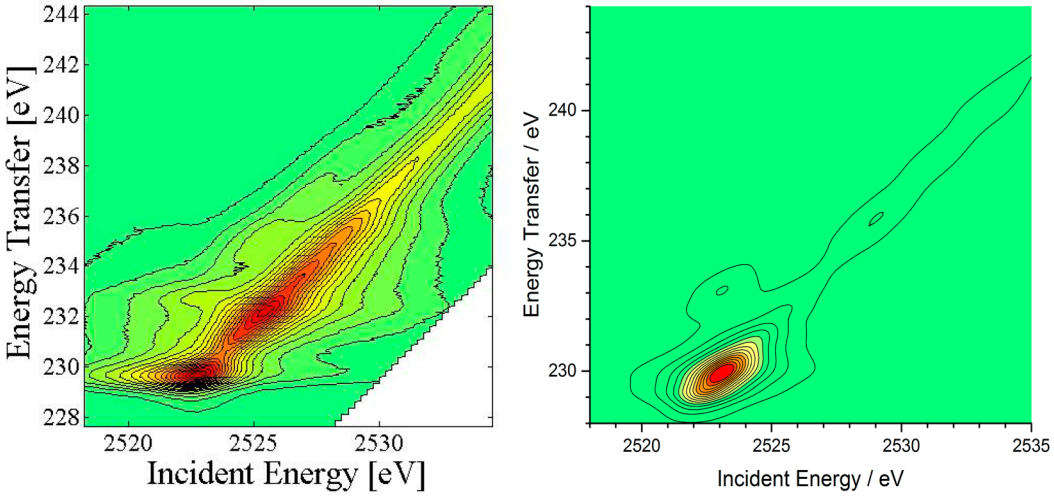

Figure 8. Experimental Lα RIXS plot (left) for MoO_2 with theoretical RIXS plot calculated using FEFF (right) for the same compound.

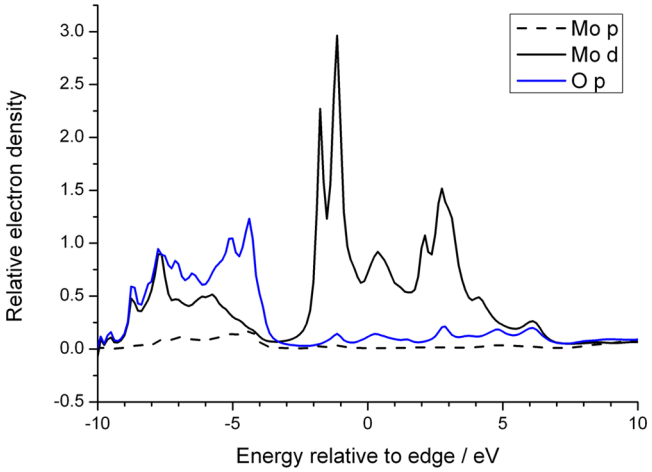

Figure 9. Density of states for MoO_2 as calculated by FEFF9.

RIXS spectra for MoS_2 as a contour plot. The main peak is split into two features; one at 2523.0 eV incident energy and 229.76 eV energy transfer, and the other at 2524.00 eV incident energy and 230.58 eV energy transfer (both are $2p_{3/2}$ to 4d; $3d_{5/2}$ to $2p_{3/2}$ transitions with 4d splitting). There are additional peaks approximately 3 eV higher in the energy transfer direction, these are due to 3d spin orbit coupling. They are weaker than in the other spectra. The density of states is shown in Figure 11, which agrees well with DOS schemas reported in literature.[25]

DISCUSSION

The RIXS spectra as obtained in this study show the clear advantage over normal L edge XANES studies in their ability to completely resolve the features present, as well as revealing new features in the RIXS planes. The features at lower energy transfer, corresponding to a $3d_{5/2}$ final state core−hole, are intense features. The higher energy transfer peaks, corresponding to a $3d_{3/2}$ final state core−hole, are weak for all samples. This is mostly due to the different transition probability of M_4 compared to M_5 emission, as mentioned (9:1 theoretically). The intensity ratio however varies across our four compounds. For example in the tetrahedral d^0 Na_2MoO_4 we see more intense and better-resolved off-diagonal peaks than the other three compounds. This is mostly due to the counting statistics, where in tetrahedral compounds there are six electrons in the higher energy t_{2g} orbitals compared to four electrons in the

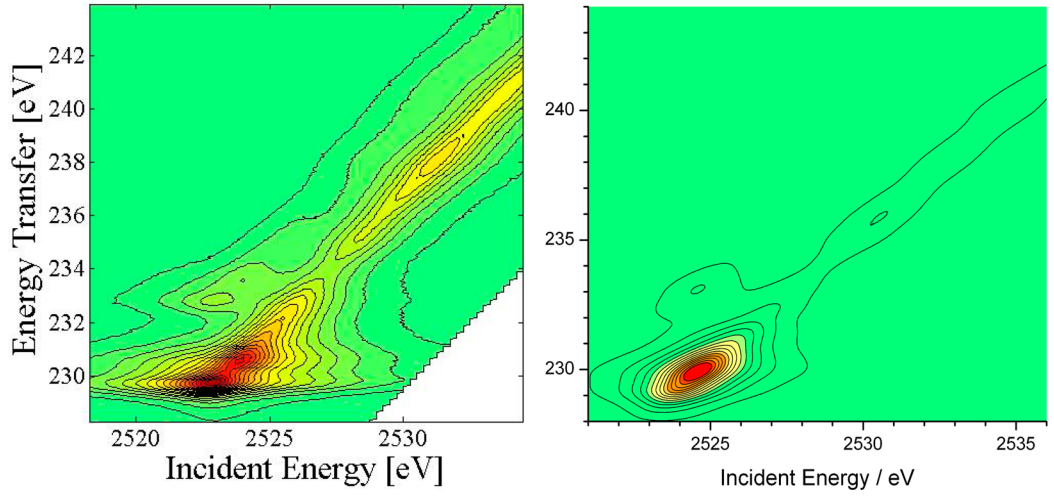

Figure 10. Experimental Lα RIXS plot (left) for MoS_2 with theoretical RIXS plot calculated using FEFF (right) for the same compound.

DOI: 10.1021/jp509376q
J. Phys. Chem. C 2015, 119, 2419−2426

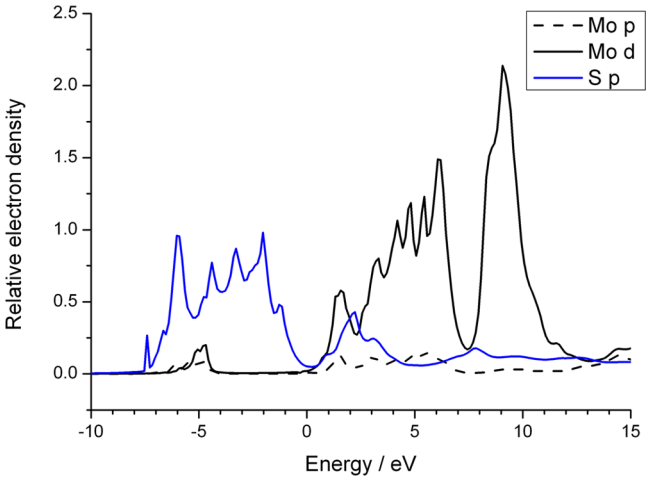

Figure 11. Density of states plot for MoS_2 as calculated by FEFF9.

lower energy e_g; see Figure 2. For octahedral compounds this is exactly the reverse.

The intensity ratio between the two main white line features in the diagonal of the RIXS plane, as also seen in an L edge absorption experiment, albeit less-resolved, is not the perfect and predicted 2:3 or 3:2 as based upon ideal tetrahedral and octahedral geometry (Figure 2). The main reason for this, as reproduced by the simulations and shown in the DOS plots, is the orbital hybridization with ligands, i.e., overlap of ligand orbitals with the metal 4d, thereby changing the density of states structure and intensity. For the tetrahedral complex the ligand O p orbital only hybridized with the first main feature, i.e., the first d orbital, and not with the second, whereas for the other (distorted) octahedral complexes, hybridization with all Mo d orbitals was observed at different intensities per orbital.

In Table 1 some important features of the RIXS spectra are summarized. A clear trend can be seen with the position of the first peak, which is clearly ∼2523 eV incident energy and ∼232 eV energy transfer for the Mo(IV) compounds, and ∼2535 and ∼230 eV for the Mo(VI) compounds. The RIXS, compared to the L edge absorption edge, allows a more reliable oxidation state determination since the features are now fully resolved. Clearly the difference in ligand type is small for the set of samples discussed here, with either oxygen or sulfur.

The 3d splitting is the spin−orbit coupling and this is very similar for all complexes, it being the 3d spin−orbit coupling which is fully shielded in the 4d transition metal. The 4d splitting reflects the sample geometry and is sample and geometry dependent. The 4d splitting for the tetrahedral complex is clearly lower than the distorted octahedral complexes, which is expected. The crystal field splitting for a tetrahedral complex will be $\sim^4/_9$th of the size of the crystal field splitting for an octahedral complex, for atomic systems assuming perfect symmetry, but the distortion of the octahedral geometry here will affect the ratio, as well as ligand hybridization, influencing the electron density of the molecular orbitals.

CONCLUSIONS

As can be seen from the experimental 2p3d RIXS plots, we can obtain greater spectral resolution compared to the L_3 fluorescence yield XANES and as a consequence can provide more accurate electronic structure information, e.g., orbital splitting and population. It also reveals additional off diagonal features that are not visible with XANES, giving insights in the geometry of the complex. The spectra can be simulated using FEFF9, with good agreement in number and relative positions of peaks, since the multiplet effects have little influence on these spectra.

These same techniques can be applied to a wide range of materials in order to obtain detailed electronic and geometric information under in situ and operando conditions. For unknown structures and changing materials the RIXS planes can be used as a direct measure for accurate oxidation states, geometry and crystal field splitting, thereby giving insights in possible ligands present. For the Mo Lα RIXS specifically, due to the relatively low X-ray energies used, special experimental cells have to be developed to allow these measurements in reduced atmosphere chambers.

ASSOCIATED CONTENT

Supporting Information

Energy transfer line scans of the experimental $L_{\alpha 1}$ RIXS plot for Na_2MoO_4 (Figure S1). This material is available free of charge via the Internet at http://pubs.acs.org.

AUTHOR INFORMATION

Corresponding Author

*(M.T.) E-mail: m.tromp@uva.nl. Present address: Van't Hoff Institute for Molecular Sciences (HIMS), University of Amsterdam, P.O. Box 94215, 1090 GE Amsterdam, The Netherlands.

Notes

The authors declare no competing financial interest.

ACKNOWLEDGMENTS

The ESRF is gratefully acknowledged for provision of beamtime under long term project CH2681. M.T. and R.T. acknowledge the EPSRC (Advanced Research Fellowship EP/E060404/1) for funding.

REFERENCES

(1) Glatzel, P.; Sikora, M.; Smolentsev, G.; Fernández-García, M. Hard X-Ray Photon-In Photon-Out Spectrocopy. *Catal. Today* **2009**, *145*, 294−299.

(2) Kotani, A.; Shin, S. Resonant Inelastic X-Ray Scattering Spectra for Electrons in Solids. *Rev. Mod. Phys.* **2001**, *73*, 203−246.

Table 1. Summary of the Molybdenum RIXS Spectra

compound	formal oxidation state	IE and ET position of first peak/eV	3d splitting−spin orbit coupling/eV	geometry	4d splitting−ligand field splitting 10*Dq*/eV
Na_2MoO_4	Mo(VI)	2524.75; 231.66	3.1	tetrahedral	2.93
MoO_3	Mo(VI)	2525.25; 231.90	3.1	distorted octahedral	3.58
MoO_2	Mo(IV)	2522.75; 229.62	2.8	distorted octahedral, short M−M bond	3.81
MoS_2	Mo(IV)	2523.00; 229.76	3.2	trigonal prismatic	1.29

DOI: 10.1021/jp509376q
J. Phys. Chem. C 2015, 119, 2419−2426

(3) de Groot, F. M. F.; Glatzel, P.; Bergmann, U.; van Aken, P. A.; Barrea, R. A.; Klemme, S.; Hävecker, M.; Knop-Gericke, A.; Heijboer, W. M.; Weckhuysen, B. M. 1s2p Resonant Inelastic X-Ray Scattering of Iron Oxides. *J. Phys. Chem. B* **2005**, *109*, 20751−20762.
(4) Kotani, A.; Matsubara, M.; Uozumi, T.; Ghiringhelli, G.; Fracassi, F.; Dallera, C.; Tagliaferri, A.; Brookes, N. B.; Braicovich, L. Theoretical and Experimental Study of Resonant Inelastic X-Ray Scattering for NiO. *Radiat. Phys. Chem.* **2006**, *75*, 1670−1675.
(5) Glatzel, P.; Singh, J.; Kvashnina, K. O.; van Bokhoven, J. A. In Situ Characterization of the 5d Density of States of Pt Nanoparticles upon Adsorption of CO. *J. Am. Chem. Soc.* **2010**, *132*, 2555−2557.
(6) Glatzel, P.; Bergmann, U. High Resolution 1s Core Hole X-Ray Spectroscopy in 3d Transition Metal Complexes − Electronic and Structural Information. *Coord. Chem. Rev.* **2005**, *249*, 65−95.
(7) Glatzel, P.; Yano, J.; Bergmann, U.; Visser, H.; Robblee, J. H.; Gu, W.; de Groot, F. M. F.; Cramer, S. P.; Yachandra, V. K. Resonant Inelastic X-ray Scattering (RIXS) at the MnK Absorption Pre-edge − a Direct Probe of the 3d Orbitals. *J. Phys. Chem. Solids* **2005**, *66*, 2163−2167.
(8) Meyer, D. A.; Zhang, X.; Bergmann, U.; Gaffney, K. J. Characterization of Charge Transfer Excitations in Hexacyanomanganate(III) with Mn K-edge Resonant Inelastic X-Ray Scattering. *J. Chem. Phys.* **2010**, *132*, 134502.
(9) George, S. J.; Drury, O. B.; Fu, J.; Friedrich, S.; Doonan, C. J.; George, G. N.; White, J. M.; Young, C. G.; Cramer, S. P. Molybdenum X-Ray Absorption Edges from 200 to 20,000 eV: The Benefits of Soft X-Ray Spectroscopy for Chemical Speciation. *J. Inorg. Biochem.* **2009**, *103*, 157−167.
(10) Bare, S. R.; Mitchell, G. E.; Maj, J. J.; Vrieland, G. E.; Gland, J. L. Local Site Symmetry of Dispersed Molybdenum Oxide Catalysts − XANES at the Mo $L_{2,3}$-Edges. *J. Phys. Chem.* **1993**, *97*, 6048−6053.
(11) Evans, J.; Mosselmans, J. F. W. L-Edge Studies on Molybdenum. *J. Phys. Chem.* **1991**, *95*, 9673−9376.
(12) Aritani, H.; Tanaka, T.; Funabiki, T.; Yoshida, S.; Eda, K.; Sotani, N.; Kudo, M.; Hasegawa, S. Study of the Local Structure of Molybdenum-Magnesium Binary Oxides by Means of Mo L_3-Edge XANES and UV-Vis Spectroscopy. *J. Phys. Chem.* **1996**, *100*, 19495−19501.
(13) Hu, H.; Wachs, I. E.; Bare, S. R. Surface-Structures of Supported Molybdenum Oxide Catalysts − Characterization by Raman and Mo L_3-Edge XANES. *J. Phys. Chem.* **1995**, *99*, 10897−10910.
(14) Hu, H.; Wachs, I. E. Catalytic Properties of Supported Molybdenum Oxide Catalysts − In-Situ Raman and Methanol Oxidation Studies. *J. Phys. Chem.* **1995**, *99*, 10311−10922.
(15) Ikeno, H.; de Groot, F. M. F.; Stavitski, E.; Tanaka, I. Multiplet Calculations of $L_{2,3}$ X-Ray Absorption Near-Edge Structures for 3d Transition-Metal Compounds. *J. Phys.: Condens. Matter.* **2009**, *21*, 104208.
(16) de Groot, F. Multiplet Effects in X-Ray Spectrocopy. *Coord. Chem. Rev.* **2005**, *249*, 31−63.
(17) de Groot, F. M. F.; Hu, Z. W.; Lopez, M. F.; Kaindl, G.; Guillot, F.; Tronc, M. Differences Between L_3 and L_2 X-Ray Absorption Spectra of Transition Metal Compounds. *J. Chem. Phys.* **1994**, *101*, 6570−6576.
(18) Kas, J. J.; Rehr, J. J.; Soininen, J. A.; Glatzel, P. Real-Space Green's Function Approach to Resonant Inelastic X-Ray Scattering. *Phys. Rev. B* **2011**, *83*, 235114.
(19) Kavčič, M.; Budnar, M.; Mühleisen, A.; Gasser, F.; Žitnik, M.; Bučar, K.; Bohinc, R. Design and Performance of a Versatile Curved-Crystal Spectrometer for High-Resolution Spectroscopy in the Tender X-Ray Range. *Rev. Sci. Insrum.* **2012**, *83*, 033113.
(20) Mårtensson, N.; Nyholm, R. Electron Spectroscopic Determinations of M and N Core-Hole Lifetimes for the Elements Nb-Te (Z = 41−52). *Phys. Rev. B* **1981**, *24*, 7121−7134.
(21) Stavitski, E.; de Groot, F. M. F. The CTM4XAS Program for EELS and XAS Spectral Shape Analysis of Transition Metal L Edges. *Micron* **2010**, *41*, 687−694.
(22) Fuggle, J. C.; Mårtensson, N. Core-Level Binding Energies in Metals. *J. Electron Spectrosc. Relat. Phenom.* **1980**, *21*, 275−281.
(23) Brandt, B. G.; Skapski, A. C. A Refinement of the Crystal Structure of Molybdenum Dioxide. *Acta Chem. Scand.* **1967**, *21*, 661−672.
(24) Wildervanck, J. C.; Jellinek, F. Preparation and Crystallinity of Molybdenum and Tungsten Sulfides. *Z. Anorg. Allg. Chem.* **1964**, *328*, 309−318.
(25) Raybaud, P.; Hafner, J.; Kresse, G.; Toulhoat, H. Ab-Initio Density Functional Studies of Transition-Metal Sulphides: II. Electronic Structure. *J. Phys.: Condens. Matter* **1997**, *9*, 11107.

DOI: 10.1021/jp509376q
J. Phys. Chem. C 2015, 119, 2419−2426